

# Highly substituted decoupled gelatin methacrylamide free of hydrolyzable methacrylate impurities: An optimum choice for long-term stability and cytocompatibility

Xueming Niu <sup>a,b,1</sup>, Gaia Ferracci <sup>c,1</sup>, Mian Lin <sup>a,1</sup>, Xiaona Rong <sup>a,1</sup>, Mengxiang Zhu <sup>a</sup>, Nam-Joon Cho <sup>c,\*\*</sup>, Bae Hoon Lee <sup>a,b,\*</sup>

<sup>a</sup> Wenzhou Institute, University of Chinese Academy of Sciences, Wenzhou, Zhejiang 325011, China

<sup>b</sup> School of Biomedical Engineering, School of Ophthalmology & Optometry, Eye Hospital, Wenzhou Medical University, Wenzhou, Zhejiang 325027, China

<sup>c</sup> School of Materials Science and Engineering, Nanyang Technological University, 639798, Singapore

## ARTICLE INFO

### Article history:

Received 21 October 2020

Received in revised form 19 November 2020

Accepted 27 November 2020

Available online 01 December 2020

### Keywords:

Decoupled gelatin methacrylamide

Methacrylate impurities

Cytocompatibility

## ABSTRACT

Gelatin methacryloyl (GelMA; GM) contains impurities, including hydrolyzable photosensitive methacrylate groups or soluble methacrylic acid (MA), which could be potentially detrimental to its *in vitro* and *in vivo* applications. To date, the influence of GM photocurable side chains on the cytotoxicity and ambient structural stability has remained to be investigated. Here, we successfully separated highly substituted decoupled gelatin methacrylamide (DGM) from GM via removing methacrylate impurities in order to evaluate its stability, cell viability, and cell toxicity, compared to GM, DGM plus soluble MA, and soluble MA. The photocurable methacrylate groups in GM were hydrolytically labile in neutral solutions, changing into soluble MA over time; on the other hand, the photocurable methacrylamide groups in DGM remained intact under the same conditions. Soluble MA was found to decrease cell viability in a dose dependent manner and caused severe cell toxicity at above 10 mg/mL. DGM plus MA started to impair cell viability at a 25 mg/mL concentration. DGM exhibited excellent cell viability and little cell toxicity across the treated concentrations (0.1–25 mg/mL). DGM without hydrolyzable methacrylate and cytotoxic MA impurities could be a better choice for long term stability and good cell compatibility for bioapplications including bioprinting and cell encapsulation.

© 2018 Elsevier B.V. All rights reserved.

## 1. Introduction

Gelatin methacryloyl (GelMA; GM) is one of the most versatile photocurable protein-based materials and has been widely used for various bioapplications, including 3D printing, regenerative medicine, drug delivery, and microchip fabrication because it offers enzyme-degradable, cell-adhesive, easy-to-handle, and stiffness-tunable properties as well as affordability [1–9]. The production of gelatin methacryloyl with consistent batch-batch quality has been established [7,10]. It has been proposed that bioapplications of gelatin methacryloyl will be close to being translated into the clinic [11,12]. Gelatin methacryloyl carries methacrylate and methacrylamide groups as photocurable side chains generated by the reaction of methacrylic anhydride (MAA)

with the hydroxyl and free amino groups of gelatin, respectively [7,9,13,14]. The separation method of decoupled gelatin methacrylamide (DGM) from gelatin methacryloyl (GM) in alkaline conditions was introduced for biomedical applications [14].

For successful clinical applications, the further understanding of the photocurable side chains of gelatin methacryloyl in terms of their ambient stability and potential cytotoxicity should be crucial. Even though photocurable gelatin methacryloyl has been extensively explored for bioapplications, the potential cytotoxicity of its degradation by-products (e.g., oligo methacrylate) and soluble impurities (e.g., methacrylic acid) has been paid little attention to and has remained to be explored [11,12,14]. Impurities generated during the gelatin methacryloyl synthesis or potential degradation methacrylate by-products produced during the storage of gelatin methacryloyl solutions (e.g., bioink products) could be potentially detrimental to cell experiments and *in vivo* applications.

The aim of this report is to investigate the ambient stability and potential cytotoxicity of photosensitive side chains of gelatin methacryloyl including methacrylate soluble impurities. Herein, we synthesized highly substituted gelatin methacryloyl (GM) bearing methacrylamide

\* Corresponding author at: Wenzhou Institute, University of Chinese Academy of Sciences, Wenzhou, Zhejiang 325011, China.

\*\* Corresponding author at: School of Materials Science and Engineering, Nanyang Technological University, 639798, Singapore

E-mail addresses: [njcho@ntu.edu.sg](mailto:njcho@ntu.edu.sg) (N.-J. Cho), [bhlee@wiucas.ac.cn](mailto:bhlee@wiucas.ac.cn) (B.H. Lee).

<sup>1</sup> These authors contributed equally to this work.

**Table 1**  
Description of samples including GM, DGM, DGM-MA, and MA.

| Sample | Description   |
|--------|---|
| GM     | Gelatin methacryloyl (Gelatin functionalized with methacrylamide groups and hydrolyzable methacrylate impurities) |
| DGM    | Decoupled gelatin methacrylamide (Gelatin methacrylamide extracted from gelatin methacryloyl)                     |
| DGM-MA | Decoupled gelatin methacrylamide containing methacrylic acid (soluble byproduct)                                  |
| MA     | Methacrylic acid  |

and methacrylate (hydrolyzable impurities) as side chains and also prepared decoupled gelatin methacrylamide (DGM; bearing only methacrylamide groups without methacrylate impurities) as well as DGM-MA containing the hydrolyzed by-product (methacrylic acid, MA; soluble impurities) as mentioned in Table 1. First, the hydrolytic susceptibility of methacrylate and methacrylamide groups in GM and DGM was examined via  $^1\text{H}$  NMR spectroscopy. Moreover, the cell viability and cell toxicity of GM, DGM, DGM-MA, and MA were investigated by cell counting kit-8 assay and lactate dehydrogenase (LDH) assays, respectively.

## 2. Materials and methods

### 2.1. Materials

Gelatin (type B, 250 bloom), sodium carbonate, sodium bicarbonate decahydrate, hydrochloric acid (HCl), sodium hydroxide (NaOH), acetohydroxamic acid, hydroxylamine, sodium dodecyl sulfate, alanine, methacrylic acid (MA), and sodium methacrylate (SM) were purchased from Aladdin (Shanghai, China). Methacrylic anhydride (MAA), iron(III) perchlorate, lithium phenyl-2, 4, 6-trimethyl-benzoyl phosphinate (LAP), and 2, 4, 6-trinitrobenzene sulfonic acid (TNBS) were purchased from Sigma-Aldrich (Shanghai, China). Deuterium oxide containing sodium-3-trimethylsilyl propionate (0.1% w/v TMSP or 0.05% w/v TMSP) were obtained from Cambridge Isotope Laboratories (Andover, USA). Dulbecco's Modified Eagle's Medium, fetal bovine serum, antibiotic/antimycotic, and Live/Dead® Cell Viability/Cytotoxicity kit were purchased from Life Technologies (Shanghai, China). Cell Counting Kit-8 (CCK-8) and Lactate Dehydrogenase-Cytotoxicity Assay Kit (LDH) were purchased from Dojindo Molecular Technologies. All the reagents were used as received.

### 2.2. Preparation of highly substituted gelatin methacryloyl (GelMA; GM) and decoupled gelatin methacrylamide (DGM)

GM and DGM were prepared similarly according to previous literature reports [7,10,14]. Briefly, type B gelatin (120 g, containing around 53.6 mmol of free amino groups) was added to 0.25 M carbonate-bicarbonate (CB) buffer (1200 mL) to be dissolved under stirring at 600 rpm at 50 °C. Methacrylic anhydride (MAA, 94%, 60 mL, 378.7 mmol) was added into the gelatin solution in a time-lapse manner (10 mL MAA addition every 10 min) with the reaction solution adjusted to pH 9.0 using a 3 N NaOH solution or a 6 M HCl solution before MAA addition. The reaction mixture was maintained at 50 °C and allowed to react for around 1 h. Then, the reaction solution was divided into two equal-volume solutions: one was adjusted to pH 7.4 to stop the reaction, filtered twice, dialyzed with a tangential flow filtration system (TFF, Darmstadt, Germany) equipped with a Pellicon® 2 cassettes (a 10 kDa Biomax® membrane, Merck Millipore) and lyophilized to obtain GM [10]. The other was allowed to further react at pH 12 at 50 °C for 0.5–1 h to remove methacrylate groups in GM, was adjusted to pH 7.4 to stop the reaction and was filtered to obtain DGM. DGM was purified in the same way as GM. GM and DGM were stored at –20 °C until further use.

### 2.3. Stability of methacrylate and methacrylamide groups in GM and DGM

GM and DGM samples were stirred at different pH solutions to monitor methacrylamide and methacrylate groups' stability in them. Each sample (2 g) was dissolved in deionized water (20 mL), and the pH was adjusted to 10, 11, or 12 using a 1 M HCl solution or a 3 N NaOH solution. Each solution at a different pH was stirred at 50 °C for 0.5 h, and then its pH was adjusted to 7.4 before lyophilization without dialysis. The samples of GM and DGM that underwent hydrolysis treatment at pH 10, 11, and 12 were denoted as GM-pH 10-0.5 h, GM-pH 11-0.5 h, GM-pH 12-0.5 h, DGM-pH 10-0.5 h, DGM-pH 11-0.5 h, and DGM-pH 12-0.5 h, respectively. GM-pH 12-0.5 h was also used as DGM-MA because methacrylate impurities in GM were expected to change into soluble methacrylic acid (MA) impurities while GM could become DGM.

To investigate the ambient stability of the photocurable functional groups in GM in a neutral solution, 40 mg of GM was dissolved in 1600  $\mu\text{L}$  of deuterium oxide containing 0.1% TMSP, which was transferred into two NMR tubes with an equal volume of the GM solution. Then, one was incubated at 37 °C for 128 days, whereas the other was incubated at 50 °C for an accelerating study.  $^1\text{H}$  NMR spectroscopy of each sample was conducted at room temperature on a Bruker Avance-I 400 MHz spectrometer (Weinheim, Germany). Phase and baseline corrections were made on all NMR spectra before integrating specific signals for quantification of the content of methacrylate and methacrylic acid (by-product) in GM [10].

### 2.4. Fe(III)-acetohydroxamic acid-based assay for quantification of methacrylate groups in GM

A series of acetohydroxamic acid (AHA) solutions in DI water ( $5.0 \times 10^{-3}$ ,  $2.5 \times 10^{-3}$ ,  $1.25 \times 10^{-3}$ ,  $6.25 \times 10^{-4}$ ,  $5 \times 10^{-4}$ , and  $2.5 \times 10^{-4}$  mol/L) were prepared and mixed with a Fe(III) solution (0.5 mol/L iron(III) perchlorate in 0.5 mol/L hydrochloric acid) at a one to one (v/v) ratio, according to the literature [10,14,15]. UV-Vis absorption spectra of the resulting solutions were recorded from 420 to 700 nm in a microplate reader with 200  $\mu\text{L}$  of a solution in each well (96-well plate). Absorbance at 500 nm was plotted against the concentration of acetohydroxamic acid to obtain a standard curve. Then, 100  $\mu\text{L}$  of a hydroxylamine hydrochloride solution (0.5 mol/L in DI water) was mixed with 100  $\mu\text{L}$  of 1 M NaOH, and then 200  $\mu\text{L}$  of a sample solution (GM of 50 mg/mL) was added to the mixed solution. The resulting solution was vortexed for 30 s and allowed to react at room temperature for 10 min. Then, 550  $\mu\text{L}$  of 0.5 M HCl was added to acidify the solution, and 50  $\mu\text{L}$  of a Fe(III) solution (0.5 mol/L iron(III) perchlorate in 0.5 mol/L hydrochloric acid) was added to the mixture solution. After it was vortexed for 30 s, the UV-Vis absorption spectra of the solution were recorded. The amount of methacrylate groups in GM samples was calculated using the standard curve (Fig. S1).

### 2.5. TNBS assay for quantification of methacrylamide groups in GM and DGM

TNBS assay was carried out as previously described [10,14,16]. Briefly, GM, DGM, and gelatin samples were separately dissolved at 1.6 mg/mL in 0.1 M sodium bicarbonate buffer. Then, 0.5 mL of each sample solution was mixed with 0.5 mL of a 0.1% TNBS solution in 0.1 M sodium bicarbonate buffer, and the mixture was incubated at 37 °C for 2 h. Next, 0.25 mL of 1 M HCl and 0.5 mL of 10 w/v% sodium dodecyl sulfate were added to stop the reaction. The absorbance of each sample was measured at 335 nm using a microplate reader. The alanine standard curve was prepared with standard solutions at 0, 0.8, 8, 16, 32, and 64  $\mu\text{g}/\text{mL}$  (Fig. S2).

## 2.6. $^1\text{H}$ NMR measurements for quantification of the methacrylamide and methacrylate groups in GM and DGM

20 mg of gelatin, GM, and DGM was separately dissolved in 800  $\mu\text{L}$  of deuterium oxide containing 0.1% w/v TMS or 0.05% w/v TMS as a chemical shift reference similarly according to the literature [10,13].  $^1\text{H}$  NMR spectroscopy of samples was conducted at 27  $^\circ\text{C}$  on a Bruker Avance-I 400 or 500 MHz spectrometers (Weinheim, Germany). Phase and baseline corrections were made on all NMR spectra before the integration of specific signals for quantification of the contents of methacrylate and methacrylamide in GM and DGM. The molar amount of methacrylate, methacrylamide, and methacrylic acid (by-product) in GM and DGM was quantified using the following formulas [10,13]. The amount of methacrylate subtracted from the amount of methacryloyl is the amount of methacrylamide.

$$\begin{aligned} &\text{The amount of methacrylate (mmol/g)} \\ &= \frac{\int \text{methacrylate (the peak at about 6.1 ppm)}}{\int \text{TMS (at 0 ppm)}} \times \frac{9\text{H}}{1\text{H}} \\ &\times \frac{n \text{ mmole (TMS)}}{m \text{ g (sample)}} \end{aligned} \quad (1)$$

$$\begin{aligned} &\text{The amount of methacryloyl (mmol/g)} \\ &= \frac{\int \text{methacryl (the peaks at 5.6–5.8 ppm)}}{\int \text{TMS (at 0 ppm)}} \times \frac{9\text{H}}{1\text{H}} \\ &\times \frac{n \text{ mmole (TMS)}}{m \text{ g (sample)}} \end{aligned} \quad (2)$$

$$\begin{aligned} &\text{The amount of methacrylic acid (byproduct, mmol/g)} \\ &= \frac{\int \text{methacrylate (the peak at about 5.3 ppm)}}{\int \text{TMS (at 0 ppm)}} \times \frac{9\text{H}}{1\text{H}} \\ &\times \frac{n \text{ mmole (TMS)}}{m \text{ g (sample)}} \end{aligned} \quad (3)$$

## 2.7. Circular dichroism analysis

To find the secondary structure of gelatin, GM, and DGM samples, circular dichroism (CD) experiments in the UV spectral range from 260 to 180 nm, were conducted using Chirascan Plus (Applied Photophysics, Leatherhead, UK) [10]. First, each sample of 0.2 mg/mL in deionized water was stored at 4  $^\circ\text{C}$  and 37  $^\circ\text{C}$  for 2 h to obtain a stable conformation of triple helix structure and random coil. The measurements were carried out at 4  $^\circ\text{C}$ , and 37  $^\circ\text{C}$  after each solution (300  $\mu\text{L}$ ) was transferred into a quartz cell with an optical path length of 1 mm.

## 2.8. Cell viability and cytotoxicity of GM, DGM, DGM-MA, and MA

Cytocompatibility of GM, DGM, DGM-MA, and MA was evaluated by culturing human hepatocellular carcinoma (HepG2) cells as a model cell. HepG2 is a cell line that has been widely used in toxicity testing [17]. Each sample of GM, DGM, DGM-MA, and MA was dissolved at 25 mg/mL in high glucose Dulbecco's modified Eagle's medium (DMEM; Gibco, Life Technologies) supplemented with 10% fetal bovine serum (FBS) and 1% antibiotic-antimycotic, and then each sample was also diluted to 20 mg/mL, 10 mg/mL, 5 mg/mL, 2.5 mg/mL, 1 mg/mL, and 0.1 mg/mL. HepG2 cells ( $4 \times 10^3$  cells/well) were seeded in 96-well tissue culture plate (TCP) and cultured in a humidified incubator at 37  $^\circ\text{C}$  with 5%  $\text{CO}_2$ . After an incubation period of 1 day, culture medium was replaced with each sample-containing medium (25 mg/mL, 20 mg/mL, 10 mg/mL, 5 mg/mL, 2.5 mg/mL, 1 mg/mL, or 0.1 mg/mL) and culture medium without samples (0 mg/mL). The cells with sample treatments were incubated for 2 days. Then, each cell medium (100  $\mu\text{L}$ ) was transferred to a new plate to test the cytotoxicity, whereas the cells remaining in the plate were treated with CCK-8 (Dojindo Molecular Technologies, Shanghai, China) to measure the cell viability [10]. Briefly,

each well with cells was incubated with a CCK solution (110  $\mu\text{L}$ : culture medium of 100  $\mu\text{L}$  plus CCK of 10  $\mu\text{L}$ ) at 37  $^\circ\text{C}$  with 5%  $\text{CO}_2$  for 2 h, and the absorbance at 450 nm was measured by a microplate reader (Thermo Fisher, USA). On the other hand, cytotoxicity was assessed using the Lactate Dehydrogenase–Cytotoxicity Assay Kit (LDH, Dojindo Molecular Technologies, Shanghai, China) according to the manufacturer's instructions [18]. Briefly, 100  $\mu\text{L}$  of LDH kit reagent was added to each well with sample medium (100  $\mu\text{L}$ ) and incubated for 10 min at room temperature, kept from light exposure. Cells treated with 0 mg/mL (without samples) was used as a negative control group, and a cell lysis buffer solution for 30 min was used as a positive control group. A microplate reader measured the absorbance at 490 nm. Also, cell morphologies in each well were examined by an optical microscope (Nikon Eclipse Ts100, Tokyo, Japan).

Besides, the cell viability of samples was semi-quantified by a Live/Dead Cell Viability/Cytotoxicity kit. HepG2 cells ( $3 \times 10^4$  cells/well) were seeded on cover slides in a 24-well tissue culture plate. After one day, the culture medium was replaced with each sample-containing medium (25 mg/mL) and control group (without samples), and the cells were further incubated for 2 days. Then, each medium was replaced with a live/dead staining solution (500  $\mu\text{L}$ ) containing 2  $\mu\text{M}$  Calcein-acetomethoxy (Calcein-AM) and 4  $\mu\text{M}$  Ethidium homodier-1 (EthD-1) and incubated at 37  $^\circ\text{C}$  with 5%  $\text{CO}_2$  for 1 h. Live (green)/dead (red) cell pictures were captured by a confocal laser scanning microscope (Nikon A1, Tokyo, Japan) [10,16]. Live and dead Cell counting was performed with ImageJ software to calculate the percentage viability.

## 2.9. Indirect cell viability and cytotoxicity of GM, DGM, DGM-MA hydrogels, and photopolymerized MA

To evaluate the indirect cell viability of GM, DGM, DGM-MA hydrogels, and photopolymerized MA, the following experiment was conducted. Each sample of GM, DGM, DGM-MA, and MA was dissolved at 100 mg/mL in PBS at 50  $^\circ\text{C}$ , and lithium phenyl-2, 4, 6-trimethylbenzoylphosphinate (LAP) was added to each sample solution at a concentration of 0.25% w/v, which was kept from light exposure. GM, DGM, DGM-MA, and MA solutions were filtered through sterile 0.2  $\mu\text{m}$  filters, and 500  $\mu\text{L}$  of each sterile sample solution was then cast in each insert with 0.8  $\mu\text{m}$  membrane in a 24 well plate before photopolymerization by UV light (365 nm; 3 mW/cm<sup>2</sup> for 10 min). In the meanwhile, HepG2 cells of  $2 \times 10^4$  were seeded into each well in a 24-tissue culture plate, and each photopolymerized sample insert was placed in the 24-well plate with cells already attached for indirect cell viability testing. Cells with each sample treatment were cultured at 37  $^\circ\text{C}$  in an incubator with 5%  $\text{CO}_2$  for 2 days. Cell viability and cytotoxicity were assessed using CCK-8 and LDH, respectively, and an optical microscope (Nikon Eclipse Ts100, Tokyo, Japan) was used to capture the cell images.

In addition, to confirm the photopolymerization of samples, each of GM, DGM, DGM-MA, and MA (100 mg) was separately dissolved in 1000  $\mu\text{L}$  of deuterium oxide ( $\text{D}_2\text{O}$ ) containing 0.05% w/v TMS. Then, 2.5 mg of photoinitiator (LAP: lithium phenyl-2, 4, 6-trimethylbenzoylphosphinate) was added to each sample solution (GM, DGM, DGM-MA, and MA), which was transferred to NMR tubes. These NMR tubes were then exposed to UV light (365 nm; 3 mW/cm<sup>2</sup>) for 10 min for photopolymerization.  $^1\text{H}$  NMR spectroscopy of samples was conducted at 27  $^\circ\text{C}$  on a Bruker Avance-I 500 MHz spectrometer (Weinheim, Germany). All NMR spectra were made to phase and baseline correction.

## 2.10. Statistical analysis

GraphPad Prism 6.01 (GraphPad Software) and Origin Pro 8.5.1 were utilized to analyze the data. The data are expressed as mean  $\pm$  standard deviation. Comparisons between the two samples were made using a

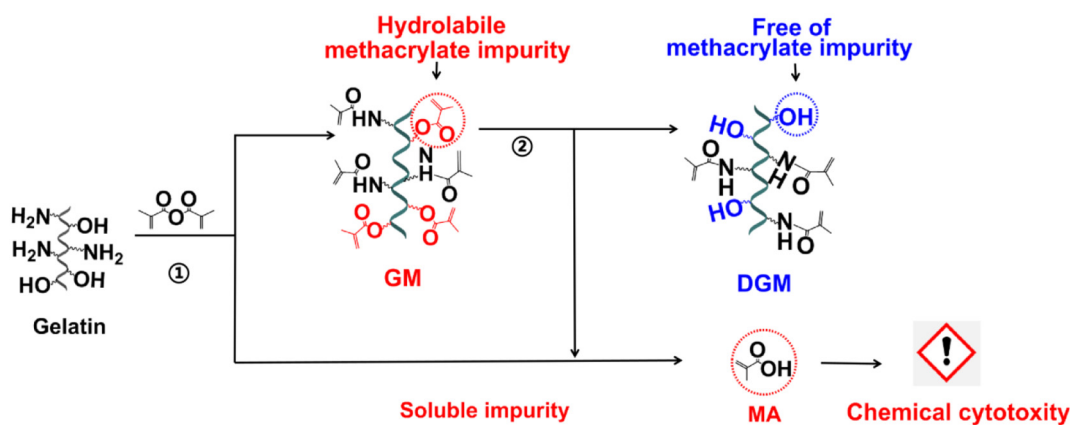


**Fig. 1.** The preparation procedure of highly substituted gelatin methacryloyl (GM) and its decoupled gelatin methacrylamide (DGM). GM was synthesized by adding methacrylic anhydride (MAA) at 50 °C in a time-lapse manner to a 10% gelatin solution and stirring in a 0.25 M carbon-bicarbonate (CB) buffer system (pH 9) for 1 h and included two photocurable groups (methacrylamide and hydrolyzable methacrylate impurities). DGM was obtained by decoupling gelatin methacrylamide from GM via additional reaction in a 0.25 M CB buffer system of pH 12 for 0.5–1 h at 50 °C and contained only methacrylamide groups without any methacrylate impurities and soluble methacrylic acid (MA).

two-tailed pair student's *t*-test. A one-way ANOVA was performed to test for differences among at least three groups. *P* values less than 0.005 were considered statistically significant, and the value of *n* denotes the number of samples or the number of experimental trials.

### 3. Results and discussion

#### 3.1. Preparation of highly substituted GM containing methacrylamide and methacrylate and DGM without any trace level of methacrylate impurities

As seen in Fig. 1, highly substituted GM with methacrylamide and methacrylate groups was prepared similarly according to previous reports [9,10,14]. DGM, without any trace levels of methacrylate impurities, was decoupled from GM via additional pH treatment. The methacrylamide and methacrylate groups in GM and DGM were quantified via NMR spectroscopy, TNBS assay, and Fe(III)-hydroxamic acid-based assay (Fig. 2A, B, C, and D), and their results are summarized in Fig. 2A. GM had both methacrylate ( $0.5520 \pm 0.0020$  mmol/g from Fe (III) assay) and methacrylamide groups ( $0.3184 \pm 0.0015$  mmol/g from TNBS assay), whereas DGM has mainly methacrylamide groups ( $0.3179 \pm 0.0029$  mmol/g from TNBS assay). The results of NMR spectroscopy showed a similar trend to those of colorimetric assays.  $^1\text{H}$  NMR spectra clearly show the specific peaks of methacrylate ( $0.5016 \pm 0.0053$  mmol/g) and methacrylamide ( $0.3800 \pm 0.0069$  mmol/g) groups in GM; one proton (1H) of the acrylic protons ( $\text{CH}_2=\text{C}(\text{CH}_3)\text{COO}^-$ ) of methacrylate appeared at around 6.1 ppm, and the other proton (1H) of the acrylic protons ( $\text{CH}_2=\text{C}(\text{CH}_3)\text{COO}^-$ ) of methacrylate and one proton (1H) of the acrylic protons ( $\text{CH}_2=\text{C}(\text{CH}_3)\text{CONH}-$ ) of methacrylamide were overlapped between 5.7 and 5.6 ppm. In addition, the methyl protons (3H) of the methacrylamide ( $\text{CH}_2=\text{C}(\text{CH}_3)\text{CONH}-$ ) and the methyl protons (3H) of methacrylate ( $\text{CH}_2=\text{C}(\text{CH}_3)\text{COO}^-$ ) appeared to be overlapped at around 1.9 ppm. On the other hand, DGM exhibited the specific peaks only belonging to methacrylamide groups ( $0.3838 \pm 0.0062$  mmol/g), as presented in Fig. 2D, indicating that the methacrylate groups in DGM were removed, and DGM bears pure gelatin methacrylamide groups as photocurable side chains.

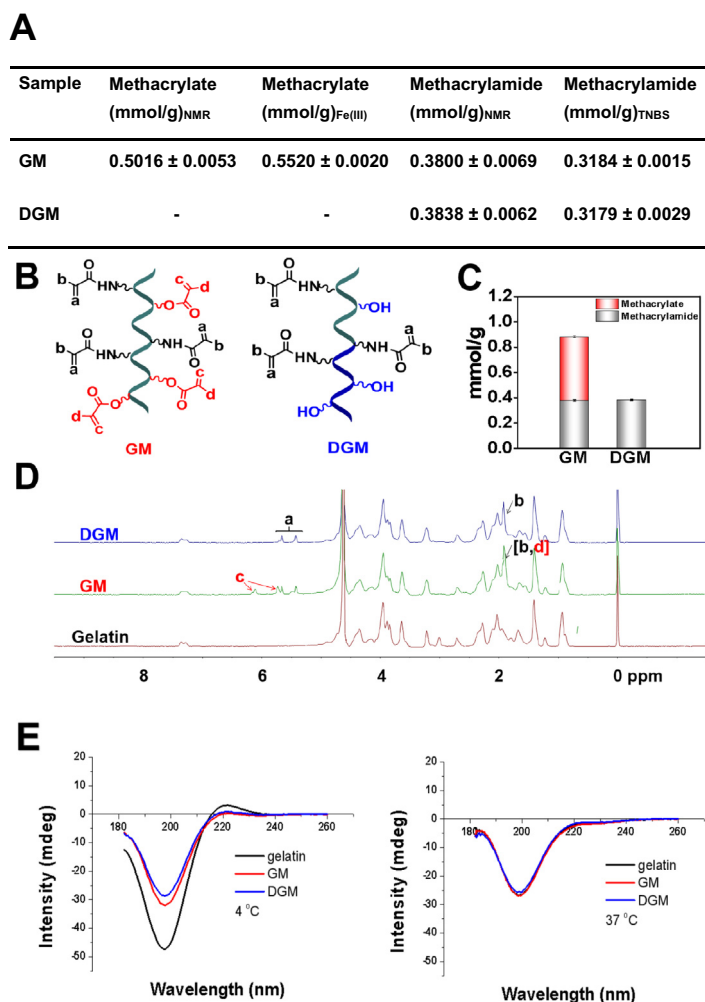
In addition, CD spectra of gelatin, GM, and DGM provided the secondary structure information at different temperatures, as depicted in Fig. 2E. GM and DGM exhibited a high rise in the intensity at 199 nm at 4 °C, relative to gelatin, implying that the methacryloyl modification of GM and DGM could increase the random coil conformation [10,19]. The difference between GM and DGM samples at 199 nm was relatively marginal. The triple-helix content of GM and DGM at 222 nm was close to each other: GM and DGM retained a low amount of the triple-helix formation at 4 °C, as compared with gelatin. On the other hand, all

samples displayed the same pattern in the CD spectra at 37 °C for all of them lost the triple helix formation and appeared to have a random coil structure at 37 °C [19].

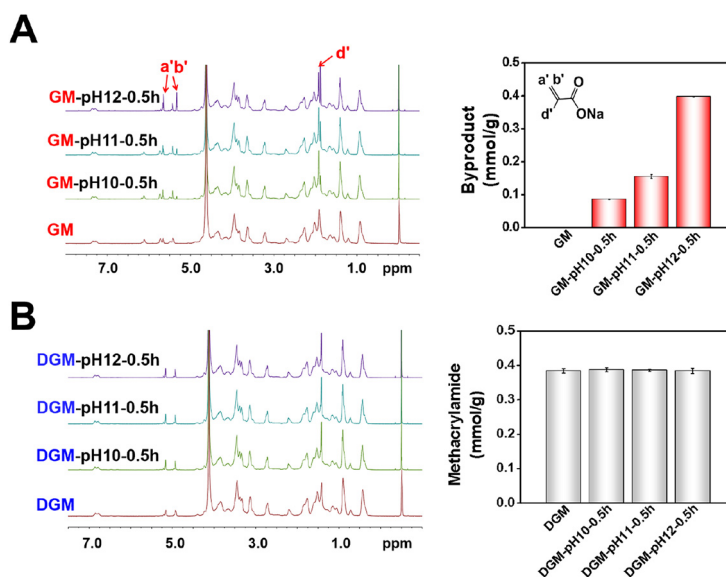
#### 3.2. The side chain stability of methacrylamide and methacrylate in GM and DGM

Fig. 3 shows the side chain stability of GM and DGM in different pH solutions (pH 10, pH 11, and pH 12) at 50 °C for 0.5 h.  $^1\text{H}$  NMR spectra of hydrolyzed GM and DGM samples were recorded to verify their structural changes (Fig. 3A and B). For GM-pH10-0.5h, GM-pH11-0.5h, and GM-pH12-0.5h, the broad acrylic peaks at around 6.1 ppm and 5.8 ppm tended to decrease as the pH increased from 10 to 12, whereas the sharp peaks of a hydrolyzed product (a salt form of methacrylic acid; sodium methacrylate) at around 5.6, 5.3, and 1.8 ppm newly appeared gradually as the pH was raised from 10 to 12. At pH 12, the methacrylate groups in GM appeared to be reduced entirely to the by-product. In GM-pH12-0.5h (DGM-MA), GM became DGM and retained the full amount of soluble methacrylic acid impurities that methacrylate groups in GM changed into. As seen in the column chart (Fig. 3A), the by-product's increasing trend was observed obviously as the pH increased. In contrast, the methacrylamide peaks of DGM exhibited little change across the different pH treatments. The column chart (Fig. 3B) shows that the amount of methacrylamide in DGM remained intact in different alkaline pH solutions, indicating that DGM could securely hold the photocurable methacrylamide functional groups in even harsh conditions and could not produce any trace levels of oligomethacrylate by-products or soluble methacrylic acid impurities. In addition, as seen in Fig. S3, methacrylate groups in GM was also susceptible to an acidic condition (at pH 2 at 50 °C for 0.5 h; GM-pH2-0.5h); the broad acrylic peaks at around 6.1 ppm and 5.8 ppm slightly decreased, whereas the sharp peaks of a hydrolyzed byproduct at around 5.6, 5.3, and 1.8 ppm newly appeared. Around 44% of the methacrylate groups in GM-pH 2-0.5 h degraded into the methacrylic acid byproduct. In contrast, NMR peaks in DGM remained relatively intact under the same acidic condition. DGM-pH2-0.5h did not exhibit any byproduct peaks, implying that the methacrylamide groups in DGM is stable even in an acidic condition.

In order to test the ambient stability of photocurable groups in GM, the photocurable methacryloyl peaks of GM in  $\text{D}_2\text{O}$  at 37 °C and 50 °C (as an accelerated condition) were monitored for 128 days via NMR spectroscopy as seen in Fig. 4A and B. When the incubation temperature was at 50 °C (Fig. 4A), the acrylic peaks at 6.1 and 5.8 ppm of GM decreased with increasing the incubation time, whereas the specific peaks of a hydrolyzed by-product at 5.3 and 1.8 ppm increased gradually with increasing the incubation time. The specific peaks of



**Fig. 2.** Characterization of highly substituted GM containing methacrylamide and methacrylate groups and DGM containing mainly methacrylamide groups. (A) The amount of methacrylamide groups and methacrylate groups of GM and DGM was measured by  $^1\text{H}$  NMR spectroscopy, TNBS assay, and Fe (III) assay. (B) The structures of GM and DGM. (C) The amount of methacrylamide groups and methacrylate groups in GM and DGM was quantified by  $^1\text{H}$  NMR spectroscopy. (D)  $^1\text{H}$  NMR spectra of gelatin, GM, and DGM in  $\text{D}_2\text{O}$  (2.5 w/v%) with TMSP (0.1 w/v%) as an internal reference. (E) CD spectra of gelatin, GM, and DGM in deionized water (0.2 mg/mL) at 4 °C and 37 °C.



**Fig. 3.** Side chain stability of GM and DGM in different alkaline solutions (pH 10, pH 11, and pH 12) at 50 °C for 0.5 h. (A)  $^1\text{H}$  NMR spectra of GM with different pH treatments. Methacrylate groups in GM turned into methacrylic acid (a byproduct; probably a salt form of methacrylic acid) in different alkaline solutions (pHs 10, 11, and 12). Specific peaks of methacrylic acid in GM with different pH treatments appeared at 5.65, 5.33, and 1.88 ppm, and their heights depended on pH treatments. The methacrylate groups in GM completely changed into methacrylic acid at pH 12 for 0.5 h. (B)  $^1\text{H}$  NMR spectra of DGM with different pH treatments. Methacrylamide groups in DGM appeared stable across the different alkaline treatments at pHs 10, 11, and 12. DGM was found to exhibit neither methacrylate groups nor soluble impurities.

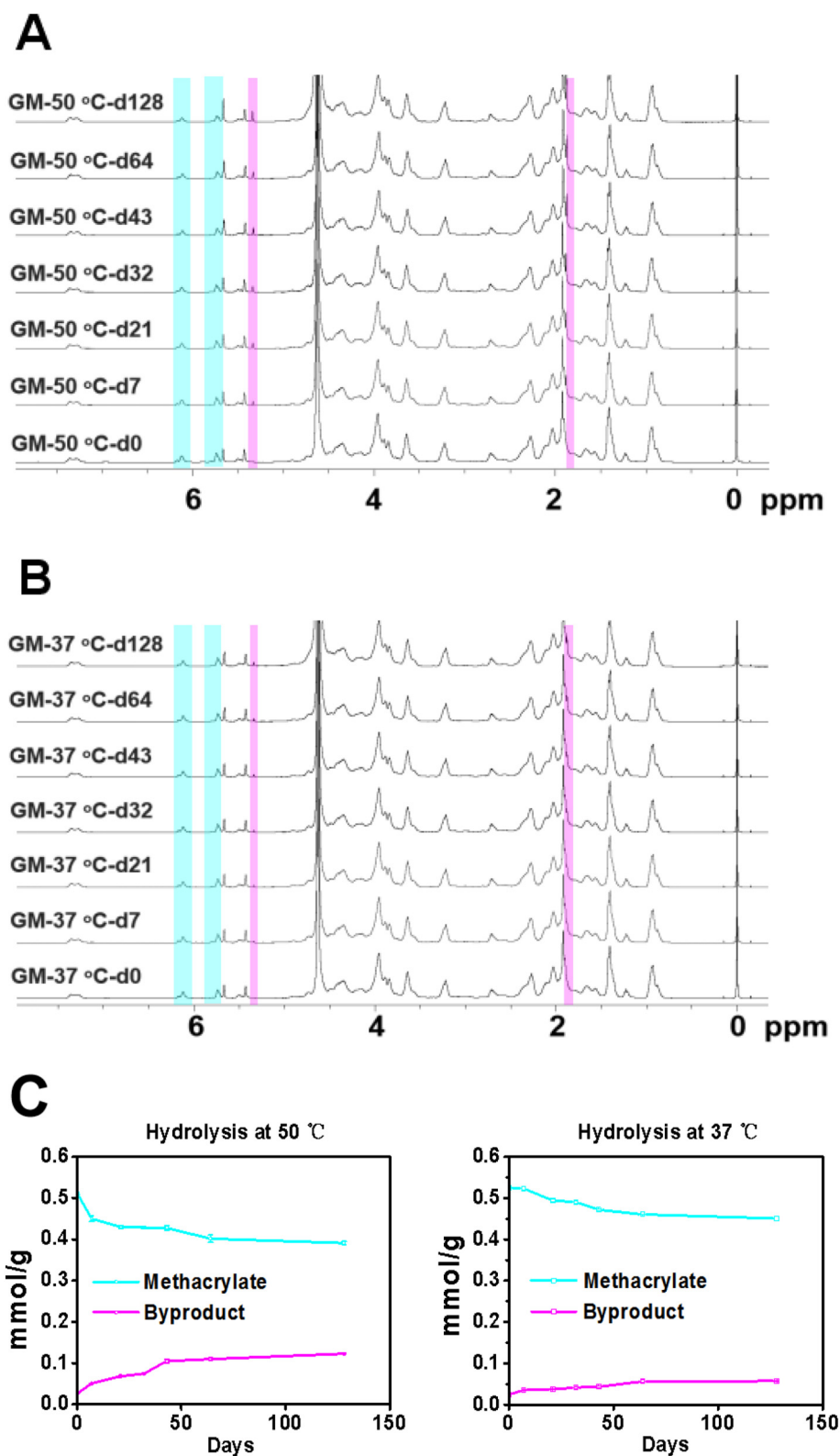


**Fig. 4.** Monitoring of the stability of methacrylate groups in GM under  $D_2O$  at 37 °C and 50 °C via NMR spectroscopy. (A), (B)  $^1H$  NMR spectra of GM under  $D_2O$  at 50 °C (A) and 37 °C (B). Specific peaks of methacrylic acid (byproduct) in GM at 50 °C and 37 °C gradually appeared at 5.65, 5.33, and 1.88 ppm. (C) Hydrolysis rate of methacrylate groups. Hydrolysis of methacrylate groups in GM was much faster at 50 °C than that at 37 °C.

methacrylic acid (by-product) started to appear on day 7. On the other hand, when the incubation temperature was at 37 °C, the overall NMR change seemed less obvious than at 50 °C, as seen in Fig. 4B. The acrylic peaks between 6.1 ppm and 5.8 ppm showed little change; however, the specific peak of a hydrolyzed by-product at

5.3 ppm started to appear on day 7 or day 21 dimly. The increase rate of the hydrolyzed by-product at 37 °C was much slower than at 50 °C during the incubation of 128 days (Fig. 4C), which indicates that the methacrylate groups in neutral solutions at 37 °C can undergo relatively slow hydrolysis.

The process of obtaining DGM from GM can potentially change the molar mass distribution of DGM and GM. GM-pH12-0.5h (DGM-MA) with the treatment at pH 12 (distilled water) for 0.5 h exhibited a weight average molecular weight of 25,096 and a polydispersity index (PDI) value of 2.14 whereas the original GM exhibited a weight average molecular weight of 21,354 and a polydispersity index of 2.19. As seen in Fig. S4, GM and GM-pH12-0.5h had a similar chromatography pattern over the similar time period, which indicates that the distilled water treatment at pH 12 for 0.5 h did little change the molar mass distribution of GM. However, DGM with the treatment of 0.25 M CB buffer at pH 12 for 0.5–1 h showed a slightly lower weight average molecular weight (Mw:15,131) and a narrower PDI value (PDI: 1.61) compared to GM and GM-pH12-0.5h, showing that the high pH buffer treatment can partially break down the backbone of GM.

### 3.3. Cell viability and cytotoxicity of GM, DGM, DGM-MA, and MA

Human hepatocellular carcinoma (HepG2) cells were used as a model cell to test the cell viability and cytotoxicity of GM, DGM, DGM-MA, and MA. HepG2 cells were cultured with respective sample solutions at different concentrations for 2 days (Fig. 5A). According to the results of the CCK-8, that reflected cell viability, GM, DGM, and DGM-MA displayed relative cell viability ranging from 73 to 130% across the treated concentrations as compared to the control group (0 mg/mL). In contrast, MA showed significantly lower cell viability (down to 5%) at concentrations from 2.5 to 25 mg/mL (Fig. 5B). Relative cell viability increased as the concentration of each GM-related sample (GM, DGM, and DGM-MA) increased from 0 to 5 mg/mL probably because gelatin-based materials can retain some bioactive sequences of collagen like arginine-glycine-aspartic acid (RGD), which can promote cell growth by integrin-mediated cell adhesion [12]. However, the relative cell viability of each GM-related sample tended to slightly decrease when each sample's concentration increased from 10 to 25 mg/mL. Especially, GM and DGM-MA solutions above 10 mg/mL tended to lower the cell viability more sharply than DGM. In addition, DGM-MA at 25 mg/mL exhibited lower cell viability (73%) than the control (0 mg/mL) without samples probably because of a critical trace level of methacrylic acid (MA; by-product). According to the calculation of the amount of methacrylic acid present in DGM-MA, DGM-MA of 25 mg/mL had an MA amount of around 1.073 mg/mL, above which the cell viability of MA could drop rapidly.

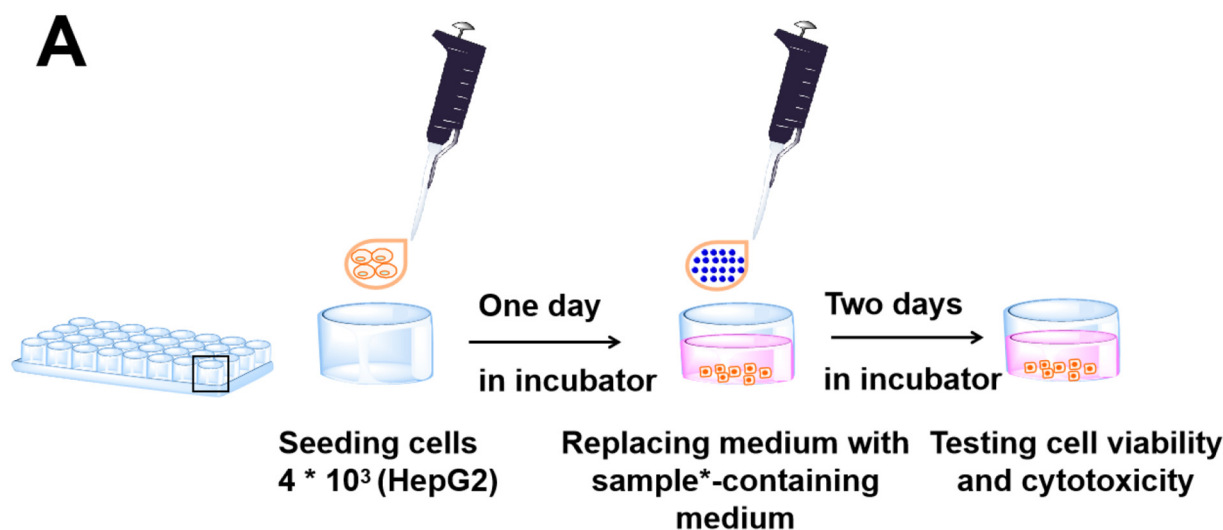
Lactate dehydrogenase (LDH) assay was conducted for cytotoxicity testing. The positive control group was treated with a cell lysis buffer, leading to complete cell death (Fig. S5), whereas the negative control group (0 mg/mL) was treated with the only culture medium. The results of the LDH assay were similar to those of CCK-8. GM, DGM, and DGM-MA exhibited low cytotoxicity across the treated concentrations. In contrast, the cytotoxicity of the HepG2 cells exposed to MA above 10 mg/mL was significantly raised compared with the zero group ( $p < 0.005$ ,  $n = 3$ ).

Fig. 5C shows optical microscope images of cells with different sample treatments. Cells treated with GM, DGM, and DGM-MA displayed rhomboid, polygonal, epithelial-like morphologies, and they grew in small aggregates, whereas the control cells treated with the cell lysis buffer lost the epithelial-like morphology completely, indicating their necrosis (Fig. S5). Moreover, cells cultivated with MA appeared to maintain their epithelial-like morphology up to a concentration of 5 mg/mL. However, these cells gradually lost their normal morphology and seemed disintegrated when the treatment concentration was over 10 mg/mL, and they no longer grew together.

In addition, the viability and toxicity of cells with different treatments were further confirmed by Live/Dead assay, as seen in Fig. 6. The cell viability of GM, DGM, and DGM-MA groups at a 25 mg/mL concentration was over 90% and was similar to that of the control group (without samples). On the contrary, no live cells (green) were observed in the MA treatment that was significantly more toxic to cells, compared to the other treatments ( $p < 0.001$ ,  $n = 3$ ).

### 3.4. The indirect cell viability and cytotoxicity of photopolymerized GM, DGM, DGM-MA, and MA

To verify the influence of photopolymerized samples on cell viability and cell toxicity, each photopolymerized sample's indirect cell viability and cytotoxicity were conducted, as presented in Fig. 7A.  $^1\text{H}$  NMR spectra of respective sample solutions containing GM, DGM, DGM-MA, and MA were recorded in Fig. 7B. In the  $^1\text{H}$  NMR spectra of polymerized GM, the methacrylic peaks ( $\text{CH}_2=\text{C}(\text{CH}_3)\text{COO}-$  and  $\text{CH}_2=\text{C}(\text{CH}_3)\text{CONH}-$ ) of methacrylate and methacrylamide groups appearing at around 6.1, 5.7, 5.4, and 1.8 ppm disappeared completely after exposure to UV light, implying that the methacrylate and methacrylamide groups in GM participated in complete photopolymerization. This photopolymerization



\* Samples - GM, DGM, DGM-MA, and MA at different concentrations.

**Fig. 5.** Cytocompatibility of GM, DGM, DGM-MA, and MA. (A) Schematic illustration of the Cytocompatibility testing of GM, DGM, DGM-MA, and MA samples. (B) Cell viability and cytotoxicity of samples at different concentrations were tested by CCK-8 and LDH assays, respectively. Results are expressed as mean  $\pm$  SD ( $n = 3$ ). \*\*\*,  $p < 0.005$ , \*\*\*\*,  $p < 0.001$  as compared to the control group (0 mg/mL). (C) Optical microscope images of cells with different sample treatments at day 2 at  $20\times$  magnification. Scale bar is 400  $\mu\text{m}$ .

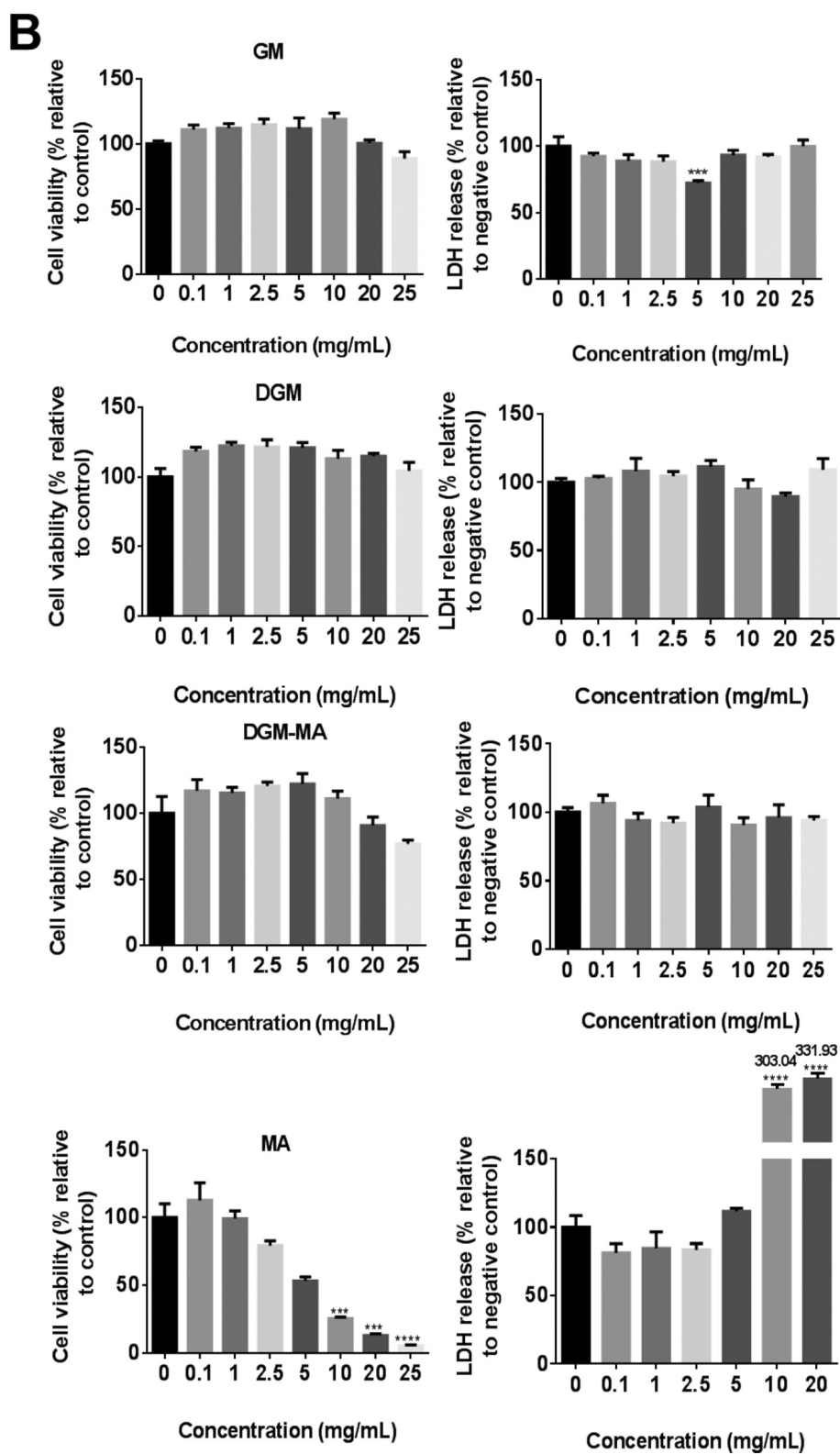


Fig. 5 (continued).



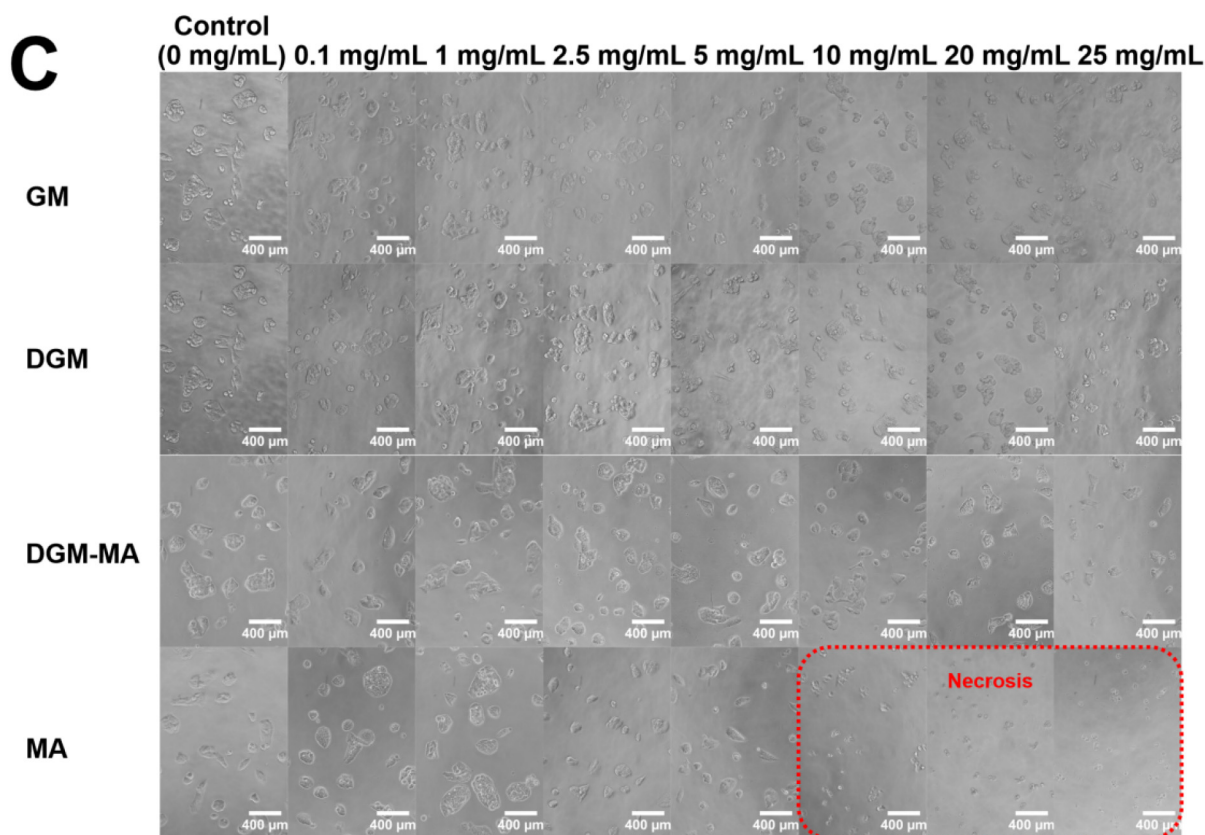
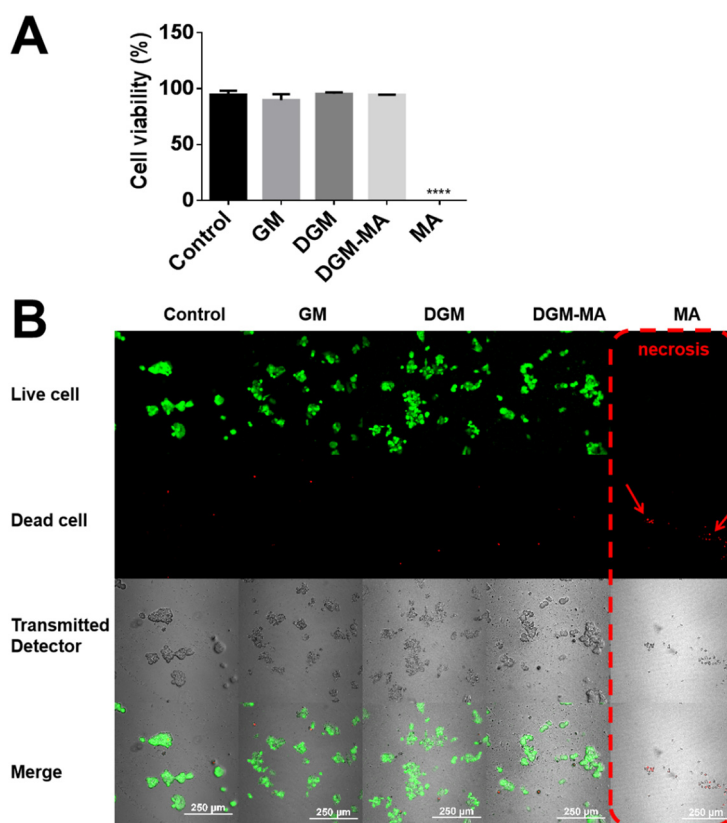


Fig. 5 (continued).



**Fig. 6.** Viability of cells with each sample treatment (25 mg/mL) was tested by Live/Dead assay kit. (A) Cell viability was expressed by counting the live and dead cells. Results are expressed as mean  $\pm$  SD (n = 3). \*\*\*\*; p < 0.001 as compared to the control group (without samples). (B) Live cells were stained green by calcein-AM, and dead cells were stained red by EthD-1. Images were taken by the confocal microscope. Scale bar is 250  $\mu$ m. (For interpretation of the references to colour in this figure legend, the reader is referred to the web version of this article.)

occurred similarly in all the samples. For photopolymerized DGM, the methacrylic peaks of methacrylamide groups appearing at around 5.4, 5.7 ppm, and 1.8 ppm disappeared because C=C bonds were reduced to single bonds by photopolymerization just as observed in the GM sample. For polymerized DGM-MA containing methacrylamide groups and methacrylic acid (probably, its salt form; sodium methacrylate), upon the exposure to UV light, methacrylic peaks belonging to methacrylamide mainly disappeared but a small proportion (around 10%) of the byproduct methacrylic peaks at 5.6, 5.3 and 1.8 ppm attributable to a salt form of MA remained unpolymerized because MA seemed more reactive to photopolymerization than its salt form (sodium methacrylate, as seen in Fig. S6).

Fig. 7C shows the results of the indirect cell viability and toxicity of GM, DGM, DGM-MA hydrogels, and photopolymerized MA. All the photopolymerized samples exhibited good cell viability and low cell cytotoxicity, even though all the photopolymerized samples were prepared at a relatively high concentration (100 mg/mL). Even a

polymerized MA sample at 100 mg/mL was not cytotoxic to cells. In contrast, the soluble monomer MA sample at 10–25 mg/mL was severely toxic to cells in the previous experiment (Fig. 5), indicating that a polymerized form of methacrylate derivatives can be less toxic to cells than their respective soluble monomer form [20,21]. In addition, a polymerized DGM sample with a small amount of unreacted MA appeared not toxic to cells. Typical polygonal morphologies of cells were observed in all the samples including the polymerized MA sample.

Gelatin methacryloyl (GM) hydrogels have been extensively investigated and utilized in a wide range of bioapplications owing to their excellent biocompatibility, the ability of enzymatic degradation, and controllable mechanical properties [1,12,15,22–26]. However, less attention was paid to the purity and cell toxicity of soluble gelatin methacryloyl precursors and the stability of photocurable side chains of GM in aqueous solutions. The preparation of pure GM free of methacrylate impurities could be crucial for clinical translation in the future [12]. Moreover, GM bioinks enclosed in a syringe are being sold in a

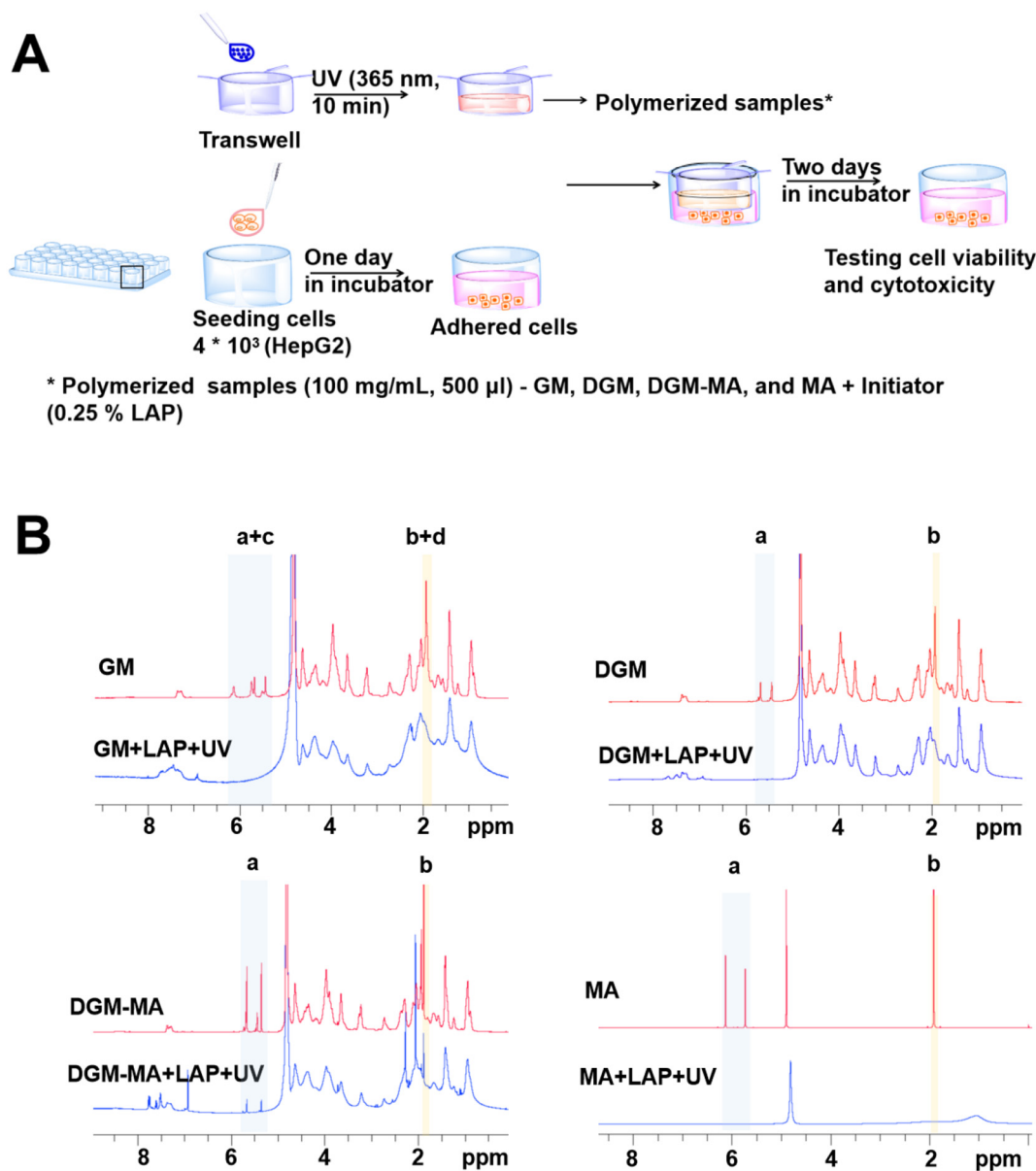


**Fig. 7.** Indirect cytocompatibility of polymerized GM, DGM, DGM-MA, and MA samples. Human hepatocellular carcinoma (HepG2) cells were seeded and one day later cells were indirectly contacted by inserts containing each sample (photopolymerized GM, DGM, DGM-MA, and MA) for 2 days. (A) Schematic illustration of the indirect cytocompatibility of photopolymerized GM, DGM, DGM-MA and MA. (B)  $^1\text{H}$  NMR spectra of GM and GM hydrogel, DGM and DGM hydrogel, DGM-MA and DGM-MA hydrogel, and MA and photopolymerized MA. LAP: lithium phenyl-2, 4, 6-trimethylbenzoylphosphinate. (C) Cell viability and cytotoxicity were tested by CCK-8 and LDH assays, respectively. (D) Optical microscope images of cells with different sample inserts at day 2. Scale bar is 400  $\mu\text{m}$ .

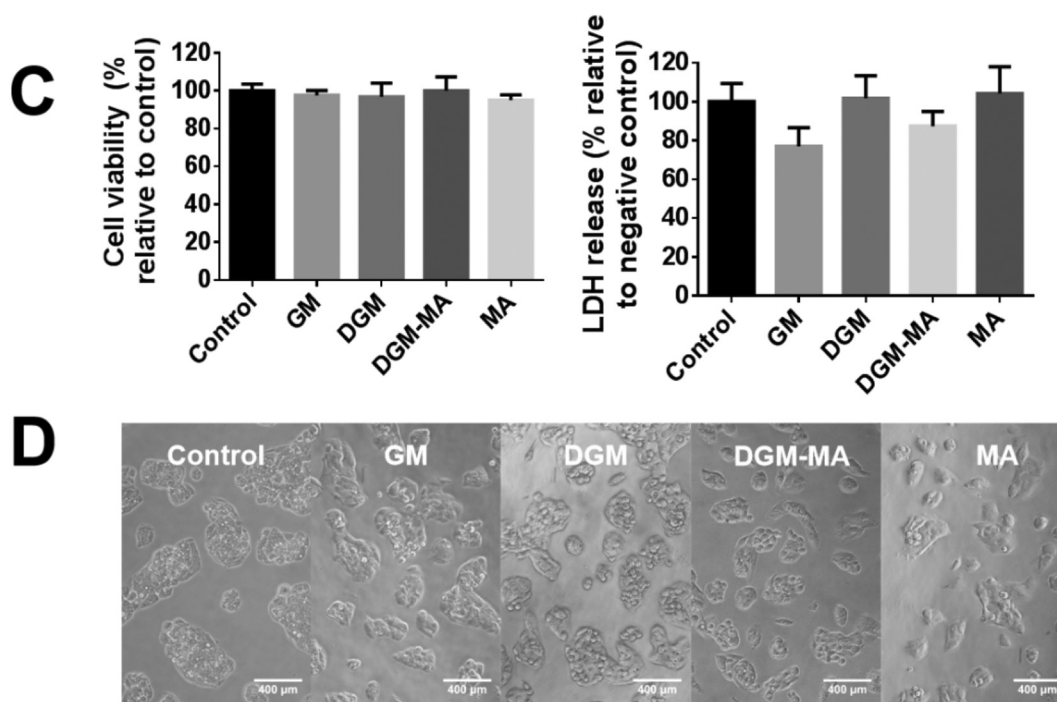


Fig. 7 (continued).

soluble state; therefore, the stability of photocurable side changes of GM bioinks in ambient conditions can be important to control their quality and to print 3D constructs with desired mechanical properties, which can rely on the photocrosslinking of available methacryloyl functional groups in GM. Methacrylate impurities in GM tend to be unstable in neutral aqueous solutions and be degraded into a corrosive by-product (methacrylic acid) over time whereas photocurable functional groups (methacrylamide) in DGM remain stable even in harsh basic and acidic conditions. DGM without hydrolysable methacrylate impurities could be useful for bioink formulations for long-term storage.

Methacrylic acid (MA) is used for paints and adhesive applications; it has been used as an adhesion nail promoter to help acrylic nails to adhere to the nail surfaces [21]. Direct contact with dilute methacrylic acid can cause tissue (skin and eyes) irritations. It was reported that the cell growth of the fibroblasts was severely impaired after the 6-day exposure to methacrylic acid (5 mmol/L; 0.430 mg/mL) [20]. In our *in vitro* (HepG2) experiments, methacrylic acid monomer at above 10 mg/mL for 2 days elicited a cell growth inhibition of more than 50%.

GM may contain various methacrylate impurities and soluble MA impurities stemming from the GM synthesis process and purification step. These impurities can affect the outcomes of GM bioapplications. Therefore, GM without these impurities could be highly desirable for *in vitro* and *in vivo* applications. DGM prepared from the two-stage process was free of methacrylate impurities and showed excellent cell viability and low cell toxicity. DGM with no trace of methacrylate and soluble MA impurities maintained the cell viability of more than 100% across the tested concentrations (0.1–25 mg/mL) whereas DGM-MA containing the fully hydrolyzed MA exhibited low cell viability (around 73%) at a concentration of 25 mg/mL, indicating that the hydrolyzed MA impurities could cause an adverse effect on cells.

#### 4. Conclusions

We successfully prepared highly substituted gelatin methacryloyl (GM) and decoupled gelatin methacrylamide (DGM) from GM via removing methacrylate impurities to compare the ambient stability of photocurable functional groups and their cell compatibility. The photocurable methacrylate groups of GM were slowly hydrolyzed into

methacrylic acid in neutral solutions at 37 °C whereas the photocurable methacrylamide groups of DGM remained stable even in harsh alkaline and acidic treatments. The photocurable groups in GM and DGM are directly related to the mechanical performance of GM and DGM hydrogels when they are cured by light. Thus, the stability of the photocurable groups in GM and DGM could be an important factor for the quality control of GM and DGM products.

GM and DGM exhibited relatively good cell viability. However, soluble byproduct methacrylic acid (MA) lowered cell viability at above 2.5 mg/mL and elicited severe cell toxicity at above 10 mg/mL. Therefore, DGM with no hydrolysable methacrylate or soluble methacrylic acid impurities could be a safer choice for *in vitro* or *in vivo* applications than GM products with hydrolysable methacrylate impurities. In addition, pure photocurable gelatin products without chemical impurities (methacrylate or methacrylic acid) as well as biological impurities (endotoxins) will be highly needed for their translational research in the future.

#### CRediT authorship contribution statement

**Xueming Niu:** Conceptualization, Investigation, Visualization, Writing-Original Draft;

**Gaia Ferracci:** Conceptualization, Investigation, Visualization, Writing-Original Draft;

**Mian Lin:** Conceptualization, Investigation, Visualization, Writing-Original Draft;

**Xiaona Rong:** Conceptualization, Investigation, Visualization, Writing-Original Draft;

**Mengxiang Zhu:** Investigation, Visualization;

**Nam-Joon Cho:** Writing-Reviewing and Editing, Supervision, Funding acquisition;

**Bae Hoon Lee:** Conceptualization, Investigation, Writing-Original Draft, Supervision, Writing-Reviewing and Editing, Funding acquisition.

#### Acknowledgments

This work was supported partly by Wenzhou Institute, University of Chinese Academy of Sciences (WIUCASQD2019003), Wenzhou Medical University (QTJ17012), the Zhejiang Provincial Natural Science

Foundation of China (LGF19E030001), and the National Research Foundation (NRF) Singapore Competitive Research Programme (NRF-CRP10-2012-070).

## Appendix A. Supplementary data

Supplementary data to this article can be found online at <https://doi.org/10.1016/j.ijbiomac.2020.11.187>.

## References

- [1] J. Zhu, X. Zhou, H.J. Kim, M. Qu, X. Jiang, K. Lee, L. Ren, Q. Wu, C. Wang, X. Zhu, P. Tebon, S. Zhang, J. Lee, N. Ashammakhi, S. Ahadian, M.R. Dokmeci, Z. Gu, W. Sun, A. Khademhosseini, Gelatin methacryloyl microneedle patches for minimally invasive extraction of skin interstitial fluid, *Small* 16 (16) (2020), e1905910.
- [2] J.R. Yu, M. Janssen, B.J. Liang, H.C. Huang, J.P. Fisher, A liposome/gelatin methacrylate nanocomposite hydrogel system for delivery of stromal cell-derived factor-1alpha and stimulation of cell migration, *Acta Biomater.* 108 (2020) 67–76.
- [3] T.J. Tigner, S. Rajput, A.K. Gaharwar, D.L. Alge, Comparison of photo cross linkable gelatin derivatives and initiators for three-dimensional extrusion bioprinting, *Biomacromolecules* 21 (2) (2020) 454–463.
- [4] K. Sakthivel, H. Kumar, M.G.A. Mohamed, B. Talebjedi, J. Shim, H. Najjaran, M. Hoorfar, K. Kim, High throughput screening of cell mechanical response using a stretchable 3D cellular microarray platform, *Small* 16 (30) (2020) e2000941.
- [5] B. Kong, Y. Chen, R. Liu, X. Liu, C. Liu, Z. Shao, L. Xiong, X. Liu, W. Sun, S. Mi, Fiber reinforced GelMA hydrogel to induce the regeneration of corneal stroma, *Nat. Commun.* 11 (1) (2020) 1435.
- [6] M. Zhou, B.H. Lee, Y.J. Tan, L.P. Tan, Microbial transglutaminase induced controlled crosslinking of gelatin methacryloyl to tailor rheological properties for 3D printing, *Biofabrication* 11 (2) (2019), 025011.
- [7] H. Shirahama, B.H. Lee, L.P. Tan, N.J. Cho, Precise tuning of facile one-pot gelatin Methacryloyl (GelMA) synthesis, *Sci. Rep.* 6 (2016), 31036.
- [8] B. Lee, N. Lum, L. Seow, P. Lim, L. Tan, Synthesis and characterization of types A and B gelatin methacryloyl for bioink applications, *Materials* 9 (10) (2016) 797.
- [9] B.H. Lee, H. Shirahama, N.J. Cho, L.P. Tan, Efficient and controllable synthesis of highly substituted gelatin methacrylamide for mechanically stiff hydrogels, *RSC Adv.* 5 (128) (2015) 106094–106097.
- [10] M. Zhu, Y. Wang, G. Ferracci, J. Zheng, N.J. Cho, B.H. Lee, Gelatin methacryloyl and its hydrogels with an exceptional degree of controllability and batch-to-batch consistency, *Sci. Rep.* 9 (1) (2019) 6863.
- [11] K. Yue, G. Trujillo-de Santiago, M.M. Alvarez, A. Tamayol, N. Annabi, A. Khademhosseini, Synthesis, properties, and biomedical applications of gelatin methacryloyl (GelMA) hydrogels, *Biomaterials* 73 (2015) 254–271.
- [12] B.J. Klotz, D. Gawlitta, A.J. Rosenberg, J. Malda, F.P. Melchels, Gelatin-methacryloyl hydrogels: towards biofabrication-based tissue repair, *Trends Biotechnol.* 34 (5) (2016) 394–407.
- [13] C. Claassen, M.H. Claassen, V. Truffault, L. Sewald, G.E.M. Tovar, K. Borchers, A. Southan, Quantification of substitution of gelatin methacryloyl: best practice and current pitfalls, *Biomacromolecules* 19 (1) (2018) 42–52.
- [14] J. Zheng, M. Zhu, G. Ferracci, N.-J. Cho, B.H. Lee, Hydrolytic stability of methacrylamide and methacrylate in gelatin methacryloyl and decoupling of gelatin methacrylamide from gelatin methacryloyl through hydrolysis, *Macromol. Chem. Phys.* 219 (18) (2018), 1800266.
- [15] K. Yue, X. Li, K. Schrobback, A. Sheikhi, N. Annabi, J. Leijten, W. Zhang, Y.S. Zhang, D.W. Hutmacher, T.J. Klein, A. Khademhosseini, Structural analysis of photocrosslinkable methacryloyl-modified protein derivatives, *Biomaterials* 139 (2017) 163–171.
- [16] G. Ferracci, M. Zhu, M.S. Ibrahim, G. Ma, T.F. Fan, B.H. Lee, N.-J. Cho, Photocurable albumin methacryloyl hydrogels as a versatile platform for tissue engineering, *ACS Appl. Bio Mater.* 3 (2) (2020) 920–934.
- [17] L. Kamalian, A.E. Chadwick, M. Bayliss, N.S. French, M. Monshouwer, J. Snoeys, B.K. Park, The utility of HepG2 cells to identify direct mitochondrial dysfunction in the absence of cell death, *Toxicol. in Vitro* 29 (4) (2015) 732–740.
- [18] S.S. Ng, A. Xiong, K. Nguyen, M. Masek, D.Y. No, M. Elazar, E. Shteyer, M.A. Winters, A. Voedisch, K. Shaw, S.T. Rashid, C.W. Frank, N.J. Cho, J.S. Glenn, Long-term culture of human liver tissue with advanced hepatic functions, *JCI Insight* 2 (11) (2017), e90853.
- [19] S.R. Shin, H. Bae, J.M. Cha, J.Y. Mun, Y.-C. Chen, H. Tekin, H. Shin, S. Farshchi, M.R. Dokmeci, S. Tang, A. Khademhosseini, Carbon nanotube reinforced hybrid microgels as scaffold materials for cell encapsulation, *ACS Nano* 6 (1) (2012) 362–372.
- [20] S. Kurata, K. Morishita, T. Kawase, K. Umemoto, Cytotoxic effects of acrylic acid, methacrylic acid, their corresponding saturated carboxylic acids, HEMA, and hydroquinone on fibroblasts derived from human pulp, *Dent. Mater. J.* 31 (2) (2012) 219–225.
- [21] P. Cosmetic Ingredient Review Expert, Final report of the safety assessment of methacrylic acid, *Int. J. Toxicol.* 24 (Suppl. 5) (2005) 33–51.
- [22] M. Sirova, S. Van Vlierberghe, V. Matyasova, P. Rossmann, E. Schacht, P. Dubruel, B. Rihova, Immunocompatibility evaluation of hydrogel-coated polyimide implants for applications in regenerative medicine, *J. Biomed. Mater. Res. A* 102 (6) (2014) 1982–1990.
- [23] P. Xu, F. Jiang, H. Zhang, R. Yin, L. Cen, W. Zhang, Calcium carbonate/gelatin methacrylate microspheres for 3D cell culture in bone tissue engineering, *Tissue Eng. Part C Methods* 26 (8) (2020) 418–432.
- [24] T. Billiet, E. Gevaert, T. De Schryver, M. Cornelissen, P. Dubruel, The 3D printing of gelatin methacrylamide cell-laden tissue-engineered constructs with high cell viability, *Biomaterials* 35 (1) (2014) 49–62.
- [25] L.M. Ptaszek, R. Portillo Lara, E. Shirzaei Sani, C. Xiao, J. Roh, X. Yu, P.A. Ledesma, C. Hsiang Yu, N. Annabi, J.N. Ruskin, Gelatin methacryloyl bioadhesive improves survival and reduces scar burden in a mouse model of myocardial infarction, *J. Am. Heart Assoc.* 9 (11) (2020), e014199.
- [26] B.H. Lee, H. Shirahama, M.H. Kim, J.H. Lee, N.-J. Cho, L.P. Tan, Colloidal templating of highly ordered gelatin methacryloyl-based hydrogel platforms for three-dimensional tissue analogues, *NPG Asia Mater.* 9 (7) (2017) e412.